Pure Appl. Geophys. 168 (2011), 2325–2334

DOI 10.1007/s00024-011-0324-0

Pure and Applied Geophysics

The Role of Adsorbed Water on the Friction of a Layer of Submicron Particles

Charles G. Sammis,[1] David A. Lockner,[2] and Ze'ev Reches[3]

Abstract—Anomalously low values of friction observed in layers of submicron particles deformed in simple shear at high slip velocities are explained as the consequence of a one nanometer thick layer of water adsorbed on the particles. The observed transition from normal friction with an apparent coefficient near $\mu = 0.6$ at low slip speeds to a coefficient near $\mu = 0.3$ at higher slip speeds is attributed to competition between the time required to extrude the water layer from between neighboring particles in a force chain and the average lifetime of the chain. At low slip speeds the time required for extrusion is less than the average lifetime of a chain so the particles make contact and lock. As slip speed increases, the average lifetime of a chain decreases until it is less than the extrusion time and the particles in a force chain never come into direct contact. If the adsorbed water layer enables the otherwise rough particles to rotate, the coefficient of friction will drop to $\mu = 0.3$, appropriate for rotating spheres. At the highest slip speeds particle temperatures rise above 100°C, the water layer vaporizes, the particles contact and lock, and the coefficient of friction rises to $\mu = 0.6$. The observed onset of weakening at slip speeds near 0.001 m/s is consistent with the measured viscosity of a 1 nm thick layer of adsorbed water, with a minimum particle radius of approximately 20 nm, and with reasonable assumptions about the distribution of force chains guided by experimental observation. The reduction of friction and the range of velocities over which it occurs decrease with increasing normal stress, as predicted by the model. Moreover, the analysis predicts that this high-speed weakening mechanism should operate only for particles with radii smaller than approximately 1 μm. For larger particles the slip speed required for weakening is so large that frictional heating will evaporate the adsorbed water and weakening will not occur.

1. Introduction

The wall rocks of most faults are separated by one or more layers of finely-granulated rock which, in order of deceasing grain size, is called fault breccia, gouge, or cataclasite (fault zone structure has been reviewed by Ben-Zion and Sammis 2003). The possibility that this material plays an important mechanical role in the nucleation and propagation of earthquakes on a fault plane has motivated many experimental studies of the coefficient of friction of a layer of granulated rock deformed in simple shear.

In recent years, attention has focused on the problem of fault zone strength at coseismic slip rates. Many laboratory studies report a loss of frictional strength on artificial faults over some range of intermediate to high slip speeds, generally at velocities above 1 cm/s (Spray 2010). Dry gabbro experiments (Tsutsumi and Shimamoto 1997) showed two distinct drops in shear strength with increasing slip rate attributed, first, to localized flash melting at asperity contacts, then, at the highest slip speeds, total surface melt formation.

Thermal decomposition of carbonates was also shown to result in profound loss of strength as high-pressure gas was released in the fault zone (Han *et al.* 2007). Although the breakdown of carbonates requires temperatures in excess of 800°C, similar dehydration reactions are likely to occur in some phyllosilicates at more modest temperatures of 150–200°C. These dehydration reactions have been proposed as a weakening mechanism in high-speed rotary shearing experiments of disaggregated ultracataclasite from the Punchbowl fault in Southern California (Kitajima *et al.* 2010). In that study, slip velocities ranged from 0.1 to 1.3 m/s at normal stresses between 0.2 and 1.5 MPa and total displacements of 1.5–84 m. They reported a significant reduction in the coefficient of sliding friction when the slip velocity and normal stress were sufficiently high to generate calculated temperatures in excess of about 150°C.

In microstructural studies of radial sections from their deformed samples, Kitajima *et al.* (2010)

[1] Department of Earth Sciences, University of Southern California, Los Angeles, CA, USA. E-mail: sammis@usc.edu
[2] US Geological Survey, Menlo Park, CA, USA.
[3] School of Geology and Geophysics, University of Oklahoma, Norman, OK, USA.

identified four distinct structural units. The first, a compacted, slightly sheared and modified starting material, and the second, a well-foliated and sheared gouge, were similar to those observed in other low-speed experiments that produce friction coefficients near 0.6. The third unit contained microstructures consistent with fluidization and was developed only at high normal stresses and slip rates that were estimated to generate temperatures greater than 150°C. The fourth unit, which also occurred at higher temperature, represents localized shearing with extreme particle size reduction. Kitajima *et al*. (2010) proposed that this fourth unit may be responsible for reduction of the friction coefficient to values as low as 0.2. Unfortunately, temperature was not measured directly in these experiments (temperature was calculated from the work expended during the tests), nor were velocities reduced during the runs to test for reversibility of the weakening effect.

Di Toro *et al*. (2004) reported weakening at sliding speeds of 0.1–10 cm/s in room-dry novaculite (fine-grained meta-sedimentary quartz rock) samples at a normal stress of 5 MPa (data are included in Fig. 1). In these experiments surface temperatures remained below 50°C. Interestingly, Di Toro *et al*. (2004) reported only modest strength loss in a granite sample tested under similar conditions. They suggested silica gel formation as a mechanism for weakening in their experiments. They noted that flash melting is probably not responsible for the observed strength loss because a run-in of ~ 1 m was needed for weakening to occur. The flash melting mechanism is proposed to occur over slip distances comparable with the asperity contact size, which would be many orders of magnitude less than their observed weakening distances.

Reches and Lockner (2010) used a rotary shear apparatus to measure friction between room-dry, solid, granite surfaces at slip velocities ranging from 0.0001 to 1.0 m/s, and at normal stresses up to 7.0 MPa. Intensive wear between the sliding surfaces produced a layer of fine-grain rock powder between 0.1 and 0.4 mm thick, even at modest stresses and displacements. Figure 1a, shows data for Sierra White granite in which the observed coefficient of friction was dependent on the sliding velocity. Four regimes can be identified. In regime I, at velocities

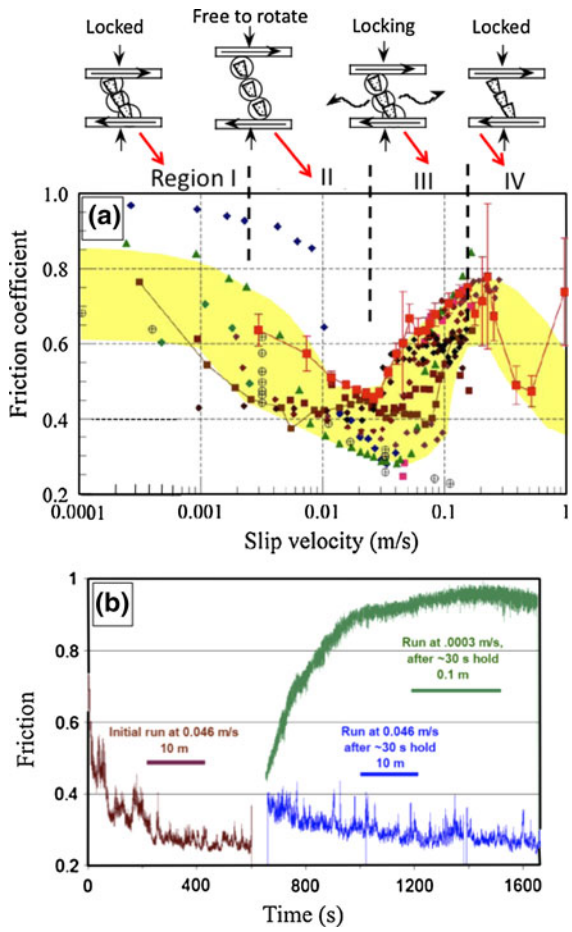

Figure 1

a The coefficient of friction as a function of slip velocity for Sierra White granite at values of the normal stress between 1 and 6.5 MPa. Some data sets are measured at increasing values of the slip velocity whereas others are measured at decreasing values. To a first-order approximation, the pattern of decreasing and values of friction is reversible. The *shaded region* (which excludes outliers) shows a general minimum in friction at slip velocities between 0.01 and 0.1 m/s for all values of normal stress, irrespective of slip direction. Four deformation regimes are identified by the *inset diagrams*, which indicate the physical conditions in each regime proposed in the text. (Modified from Reches and Lockner (2010) which contains the details of each run). **b** Two slide–hold–slide experiments on Sierra White granite. In both cases, the sliding velocity was 0.046 m/s before a 30 s hold. In the first case, the sliding velocity following the hold was again 0.046 m/s. In the second the sliding velocity following the hold was 0.0003 m/s (modified from Reches and Lockner 2010)

below about 0.001 cm/s, the coefficient μ was generally in the range 0.6–0.75, typical of values measured in other low speed experiments. In regime II, μ decreased with increasing slip velocity reaching

a minimum near $\mu = 0.3$ at slip velocities between about 0.01 and 0.05 m/s. In regime III, μ increased with increasing slip velocity returning to values in the range 0.6–0.75 at slip velocities above approximately 0.1–0.2 m/s. In regime IV, at slip speeds above approximately 0.2 m/s, the coefficient remained in the range 0.6–0.75 with a second decrease in friction at the highest slip rates in one experiment.

The strength increase in regime III was observed to correlate with a rise in the temperature of the powder layer above 120°C, which led Reches and Lockner (2010) to propose that this strengthening was caused by evaporation of adsorbed water from the gouge particles. Their observation that the weakening/strengthening response is reversible over the entire range of velocities supports their suggestion that it is caused by changes in the thin film of adsorbed water on the ultra-fine particles, and not by an evolution in grain-size or packing structure. The four diagrams above the graph in Fig. 1a illustrate our proposed mechanism for each regime, which will be developed in a later section.

Figure 1b shows the results of two slide–hold–slide experiments. In both experiments sliding was initiated at 0.046 m/s. Over a sliding distance of approximately 20 m, the coefficient of friction decreased to a value near $\mu = 0.3$, a value commonly observed for this mode II velocity. Sliding was then stopped for a hold period of approximately 30 s. In the first experiment, sliding was resumed at the same velocity of 0.046 m/s and friction decreased from $\mu = 0.4$ (its value immediately after the hold) back toward $\mu = 0.3$ (its value immediately before the hold). It is interesting that this reduction in friction after the hold requires the same 20 m. sliding displacement as the initial run-in. The implication is that 20 m of slip is required to establish an equilibrium configuration.

In the second experiment, sliding after the hold occurred at a lower velocity of 0.0003 m/s. In this case friction increased from $\mu = 0.4$ to $\mu = 0.95$ over a sliding distance of approximately 0.3 m., much shorter than the transient at the higher slip velocity. However, although the slip distances vary by a factor of 67, the time intervals for the two transients only differ by a factor of 2.3, which suggests a chemical rather than structural adjustment. On the other hand, it is possible that $\mu = 0.95$ is not the equilibrium friction coefficient, and, in fact, the coefficient seems to have peaked and is slowly decreasing by the end of the run. The shape of this curve is reminiscent of the behavior of an "over-consolidated" granular material in a shear box experiment in which the shear stress overshoots the equilibrium value until the material dilates to the equilibrium value for the applied strain rate. It is possible that the unusually high values of μ may characterize over-consolidated packing of the newly jammed particles at this low slip speed.

It is interesting to compare the Reches and Lockner (2010) results with those from the other studies discussed above. As in the Di Toro *et al.* (2004) experiments, large run-in distances make it unlikely that the flash heating inferred by Tsutsumi and Shimamoto (1997) is active in the Reches and Lockner (2010) experiments. Although Reches and Lockner (2010) did not carry out detailed microstructural studies of their slip surfaces, their observation of continual surface wear and the production of fine-grained gouge suggest that neither silica gel formation (as in Di Torro *et al.* 2004) or total surface melt (as in Tsutsumi and Shimamoto (1997) were the dominant mechanism. It is not clear how to compare the Reches and Lockner (2010) results with those of Kitajima *et al.* (2010) who, unfortunately, did not directly measure the temperature (temperature was calculated from the work expended during the tests). Also, they did not reduce sliding velocity during the runs to test for reversibility of the weakening effect.

In this paper, we quantitatively explore the Reches and Lockner (2010) hypothesis that the velocity-dependent weakening and strengthening in their experiments is associated with changes in a layer of adsorbed water on the submicron wear particles that accumulate between the sliding surfaces. We ignore possible kinetic weakening mechanisms, for example dilatation caused by momentum transfer between particles, because the observed strengthening with increased velocity in regime III is antithetical to such mechanisms. It is possible, however, that the hint of weakening at slip velocities above approximately 0.4 m/s in Fig. 1a is kinetic in origin.

2. The Effect of Adsorbed Water on Packing Density

Granular solids may be characterized by their packing density ϕ, which is defined as $\phi = (V_{\text{solid}}/V_{\text{total}})$. For spheres of similar sizes, the maximum packing density is $\phi = 0.74048$ (for either body-centered or face-centered packing). For "random close packing" capable of supporting a load, $\phi \approx 0.64$ (Kamien and Liu 2007).

If a granular mass of spheres of similar sizes is loaded in shear, flow can occur only if $\phi < \phi_c$ where ϕ_c is a critical packing density above which "jamming" occurs. When $\phi \geq \phi_c$ the particles jam and flow requires either dilation of the mass or fracture of the particles to free individual jams. The critical value of the packing parameter has been measured to be $\phi_c = 0.576 \pm 0.004$ (Brown and Jaeger 2009).

Based on measurements of the particle sizes and the bulk adsorption of water, Reches and Lockner (2010) estimated the thickness of the adsorbed water layer, δ, to be approximately four monolayers, or approximately 1 nm. We now ask, how small must the spheres be for an adsorbed layer of thickness δ to be reduced ϕ from the random close packed value of $\phi = 0.64$ to the critical value of $\phi_c = 0.576$ below which flow can occur?

Consider an array of spheres of radius r with packing parameter $\phi = \frac{4}{3}\pi r^3 N_{\text{V}}$ where N_{V} is the number of spheres per unit volume. If each sphere is surrounded by a few monolayers of water of thickness δ as in Fig. 2, but the packing geometry is unchanged, the value of ϕ is reduced to $\phi' = \frac{4}{3}\pi(r-\delta)^3 N_{\text{V}}$ and we can write:

$$\frac{\phi'}{\phi} = \left(1 - \frac{\delta}{r}\right)^3 \tag{1}$$

Flow requires $\phi' \leq \phi_c$ which gives

$$\frac{\delta}{r} \geq 1 - \left(\frac{\phi_c}{\phi}\right)^{1/3} \tag{2}$$

For a granular mass that begins at random close packing the condition for flow is $r \leq 29\delta$. Because four monolayers of water correspond to $\delta \approx 1$ nm, flow requires $r \leq 29$ nm. We note that particles this small or smaller were observed by Chester *et al.* (2005) in the Punchbowl cataclasites and by Reches and Lockner (2010) in the wear products produced by their rotary shear apparatus. The apparent fluid structure observed by Kitajima *et al.* (2010) in the finest particles may be because of their subcritical packing density.

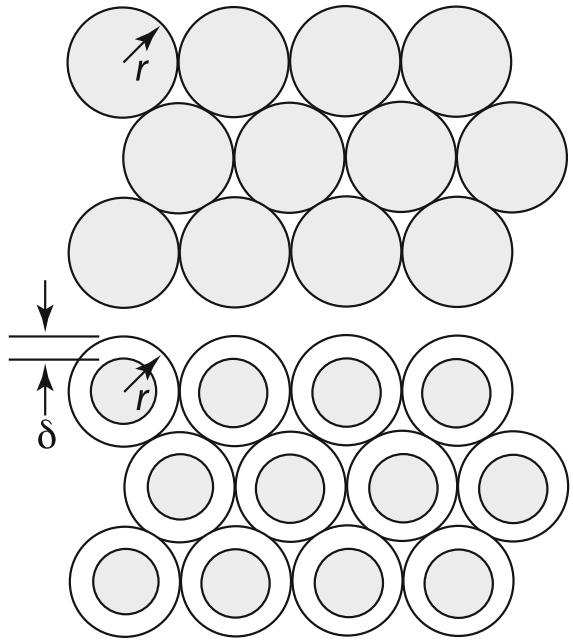

Figure 2
The *upper panel* shows an array of circles in close packing. The *lower* shows the same packing, but with the circles surrounded by an adsorbed water layer of thickness δ. Although packing is still maximized the packing density of the circles is reduced

The apparent viscosity of a fluidized layer of particles deforming near ϕ_c is very sensitive to ϕ_c. In this fluidized regime deformation is strain-weakening. Any positive strain fluctuation heats the water locally, reducing its viscosity and producing further localization. This may be the source of the extreme shear localizations observed by Kitajima *et al.* (2010), which they term "unit four".

The adsorbed water layer does not have to reduce ϕ below ϕ_c in order to produce the observed reduction in friction. It only has to produce enough separation to enable the submicron particles to rotate. Abe and Mair (2009) studied the effect of particle shape on the apparent friction of a layer of particles. Their numerical simulations found that an array of particles in the jammed state had a coefficient of friction of 0.6 if they were irregularly shaped and free to fracture. However, at the same packing density, the

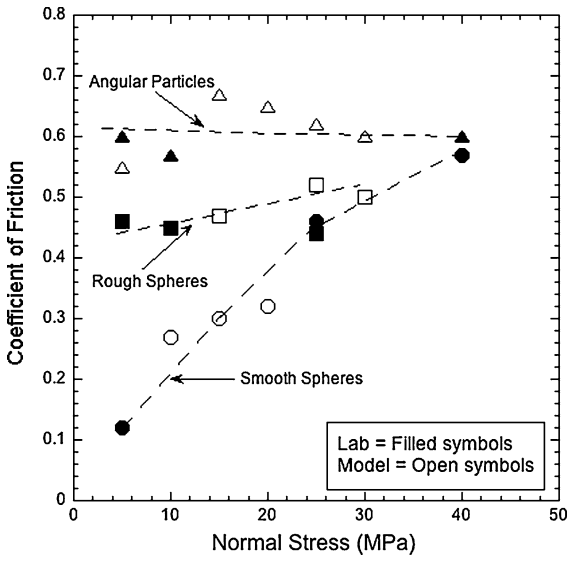

Figure 3
The coefficient of friction of rough particles compared with spheres (redrawn from ABE and MAIR 2009). Rough breakable particles in a jammed configuration tend to have a coefficient near $\mu = 0.6$. Smooth spheres in a jammed configuration tend to have a lower coefficient near $\mu = 0.3$, particularly at normal stress below 10 MPa as in the RECHES and LOCKNER (2010) experiments

coefficient of friction dropped to 0.3 if the particles were spherical and free to rotate. As illustrated in Fig. 3, these numerical results are consistent with laboratory measurements on arrays of unbreakable spheres. It may be coincidental that this is the same reduction in friction observed by RECHES and LOCKNER (2010) and by KITAJIMA *et al.* (2010)—or it may not.

In the following discussion we will use the term "locked" to characterize nearest neighbor particles that are not free to rotate. We use the common definition of "jammed" to denote a configuration with packing density above the critical value ϕ_c. Hence for a jammed configuration with locked particles we expect $\mu = 0.6$, but for a jammed configuration with unlocked particles we expect $\mu = 0.3$.

3. *Extrusion of the Adsorbed Water Layer*

Why does the adsorbed water layer only reduce the coefficient of friction at slip speeds above 0.01 m/s? That is, why doesn't the adsorbed water also lower friction at the lower slip speeds in regime *I* in Fig. 1a? One possibility is that the contact time between particles at lower slip speeds is sufficiently long that the particles penetrate the adsorbed water layer and become locked.

The stress field in a jammed granular layer is known to be very heterogeneous. The load is carried by a network of grain-bridges, or force chains that are continually forming and failing as deformation proceeds. The average lifetime of a contact between grains in a force chain, t_c, should scale with the particle radius, r, and the slip velocity v as

$$t_c = \alpha r / v \tag{3}$$

where α is an adjustable constant incorporating the thickness, structure, and temporal evolution of the network.

We wish to compare this contact time t_c with the time t_x required to extrude the adsorbed surface layer of water from between two particles in a force chain. If $t_x < t_c$ (at low sliding velocities) the water layer will be extruded during the lifetime of a contact and the particles will lock. If $t_x > t_c$ the water layer will survive the lifetime of a force chain, the particle will not lock, and rotation becomes possible.

In order to estimate t_x, we need to estimate the force carried by the chains and the viscosity of the adsorbed water layer. To estimate the force, we use the statistical description of force-chain networks in packs of spheres of similar sizes measured by MUETH *et al.* (1998). In their experiments a confined cylindrical sample (diameter = 140 mm) containing 55,000 spherical glass beads (diameter = 3.5 ± 0.2 mm) was loaded in axial compression. The force exerted by each individual bead on the top and bottom pistons and the walls of the cylinder was determined by comparing the diameter of its impression as revealed by a sheet of carbon paper with a set of calibrated impressions.

Between 800 and 1,100 contact points were observed on the surfaces of the pistons. Tests with adhesive tape revealed there were an additional 4–6% of contacting particles where the force was too low to produce an impression. Given the diameter of the pistons and the diameter of the glass spheres, these numbers translate to a surface packing density in the range 0.53–0.72, significantly less than the 0.91 expected for hexagonal packing. Figure 4 shows the

observed cumulative distribution of dimensionless forces $f \equiv F/\overline{F}$, where the forces are scaled to their mean value $\overline{F}$. Note that the probability distribution $P(f)$ decreases exponentially for $F > \overline{F}$ (or, equivalently, $f > 1$).

The average force $\overline{F}$ carried by a force chain in a granular layer that is supporting a normal stress $\sigma_n$and deforming with a macroscopic coefficient of friction μ is:

$$\overline{F} = \sigma_n A_c \sqrt{1+\mu} \tag{4}$$

where A_c is the average surface area per chain. Using an average value of the observed surface packing density gives $A_c \approx \pi r^2/0.62$ so

$$\overline{F} \approx \frac{\pi\sqrt{1+\mu}}{0.62}\sigma_n r^2 \tag{5}$$

The observed force distribution in Fig. 4 falls off so rapidly that only about one chain in ten supports a force above $F = 2\overline{F}$.

In response to this force, the adsorbed water layer will be extruded from between the particles at a rate that depends on its effective viscosity. We estimate the extrusion rate by modifying results from Dienes and Klemm (1946), who derived a modified form of Stefan's equation for the extrusion of a viscous fluid (viscosity η) from the gap between coaxial parallel circular plates of radius a as the distance between them is reduced by an axial force F

$$\frac{1}{h^2} - \frac{1}{h_o^2} = \frac{4F}{3\pi\eta a^4}t \tag{6}$$

In this equation h_o is the initial separation at time $t = 0$ and h is the final separation at time t (Fig. 5a). Note that Eq. (6) is a solution of the differential equation:

$$\frac{dh}{dt} = -\frac{8Fh^3}{3\pi\eta a^4} \tag{7}$$

for the case of constant a. We can also solve Eq. (7) to find $h(t)$ for two identical spheres being pushed together by force F. In this case the radius of contact a is a function of the radius of the spheres r, and their separation h

$$a = \sqrt{(2\delta - h)r} \tag{8}$$

where δ is the thickness of the adsorbed layer in Fig. 5b.

Substituting Eq. (8) into Eq. (7) and integrating gives the extrusion time t_x required to reduce h from an initial thickness $2\delta = 2\ m$ monolayers to a final thickness of one monolayer.

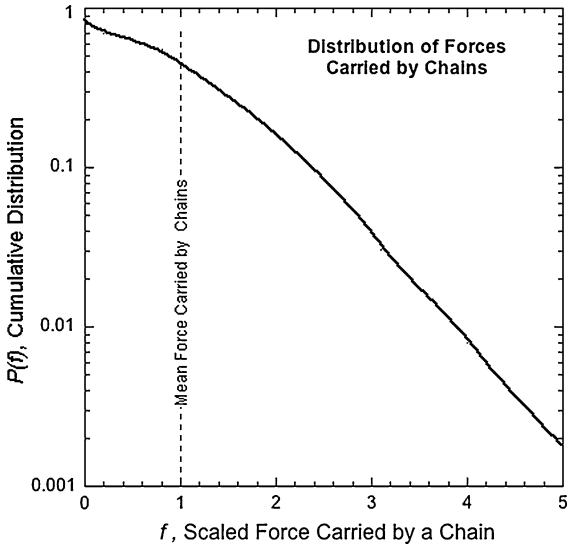

Figure 4
The distribution of forces carried by force chains measured in a cylindrical sample of monodispersed glass spheres (redrawn from Mueth *et al.* 1998)

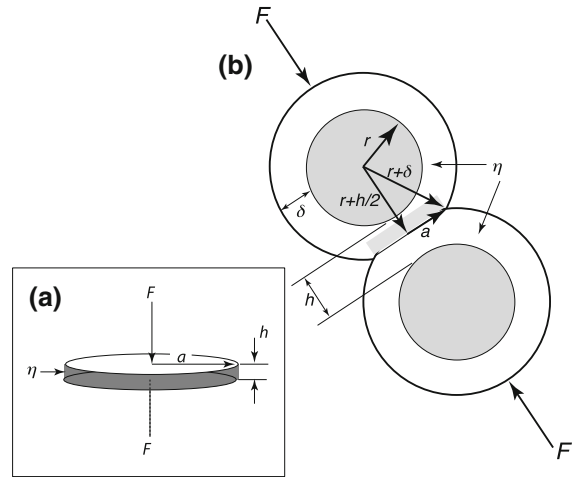

Figure 5
a Fluid with viscosity η being extruded from between coaxial circular disks by force F. **b** The contact between two solid spheres surrounded by an adsorbed water layer showing the radius of contact a

$$t_x = \frac{3\pi\eta r^2}{F}\frac{(4m^2 - 8m + 3 - 2\mathrm{In}(2m))}{16} \quad (9)$$

Because there is a distribution of forces on the chains and we do not know how many chains must lock to produce a change in the coefficient of friction, we define:

$$F_c = \beta\overline{F} = \frac{\beta\pi\sqrt{1+\mu}}{0.62}\sigma_n r^2 \quad (10)$$

where β defines a critical value of the force F_c that can be sustained by a force chain during its contact time t without extruding the water layer. Particles in chains with $F > F_c$ will lock while those in chains with $F > F_c$ have some rotational freedom.

Substituting Eq. (10) into Eq. (9) gives:

$$t_x = \frac{3}{16}\frac{4m^2 - 8m + 3 - 2\mathrm{In}(2\mathrm{m})}{\beta\sqrt{1+\mu}}\frac{\eta}{\sigma_n} \quad (11)$$

Setting $t_x = t_c$ using Eq. (3) gives:

$$v_c = \frac{16}{3(4m^2 - 8m + 3 - 2\mathrm{In}(2\mathrm{m}))}\alpha\beta\sqrt{1+\mu}\frac{\sigma_n}{\eta}r \quad (12)$$

where v_c is the critical sliding velocity above which contacts in a chain carrying force $F \le \beta\overline{F}$ remain separated by the adsorbed water layer.

The parameters in Eq. (12) were estimated as follows. Because approximately 50% of the grain bridges carry a force greater than $0.5\overline{F}$, we assume that $\beta = 0.5$ characterizes the force at which particle contact begins. We take $\sigma_n = 2$ MPa, a typical value in the Reches and Lockner (2010) measurements.

Although Reches and Lockner (2010) did not measure the particle size distribution in the wear-powder, they reported that SEM measurements found most grains are "angular and in the submicron range" ($r < 500$ nm) and that "many grains are below the 0.1 μm SEM resolution" ($r < 50$ nm). We assume here that particles as small as $r = 20$ nm exist, because they were observed in natural ultracataclasite by Chester *et al*. (2005). Note that the contact time t_c in Eq. (3) is proportional to r, so groups of the smallest particles have the shortest contact time. Because the extrusion time t_x in Eq. (11) is independent of r, the smallest particles will be the first to unlock. We therefore assumed $r = 20$ nm to calculate the critical velocity, v_c, at which the reduction in m begins. Note that this reduction (Fig. 1a) extends over at least one order of magnitude in slip velocity which may reflect the progressive unlocking of larger particles.

There is substantial uncertainty in the value of η, because the viscosity of the first few monolayers of adsorbed water is much larger than the nominal viscosity. Major *et al*. (2006) measured the viscosity of a 1 nm thick layer of adsorbed water to be $\eta = 30$ kPa s, more than seven orders of magnitude higher than the viscosity of water at room temperature ($\eta_{bulk} = 8.6 \times 10^{-4}$ Pa s) (Li *et al*. 2007). Note that in these experiments a 1 nm thick layer between the quartz surfaces corresponds to four monolayers, or two monolayers on each surface. Hence, in evaluating Eq. (12) we take $m =$ two monolayers. This high viscosity is associated with the formation of an ice-like network in the first few adsorbed monolayers as revealed by infrared spectroscopy. Asay and Kim (2005) observed that as relative humidity increased from 0 to 30% a hydrogen-bonded ice-like network of water grew to a thickness of three monolayers. Between 30 and 60% relative humidity the ice-like network grew to saturation while liquid water formed on the surface. Above 60% relative humidity liquid water continued to form on top of the ice-like structure. Israelachvili (1986) found that the apparent viscosity fell to the nominal value for water when the thickness of the adsorbed layer was 2 nm or more.

The fact that the viscosity of the adsorbed layer is so sensitive to layer thickness which, in turn, is sensitive to relative humidity, may explain the large scatter in Fig. 1a. By assuming $m = 2$ in our calculations, we assume an initial separation of $h_o =$ four monolayers, or approximately 1 nm (Fig. 5b). Although Reches and Lockner (2010) estimate an adsorbed layer thickness of approximately four monolayers and, hence, an initial $h_o =$ eight monolayers, we assume that the viscosity is low enough to be ignored until h is reduced to four monolayers.

The value of α defined by Eq. (3) is the most difficult to estimate. In the calculations plotted in Fig. 6 we treat α as adjustable and take $\alpha = 45/\sqrt{1+\mu}$ which, for the grain size ($r = 20$ nm) and critical velocity $v_c = 0.001$ m/s measured by Reches and Lockner (2010), an initial separation of $h_o = 4$ monolayers corresponds to the measured viscosity of $\eta = 30$ kPa s at a normal stress of 2 MPa.

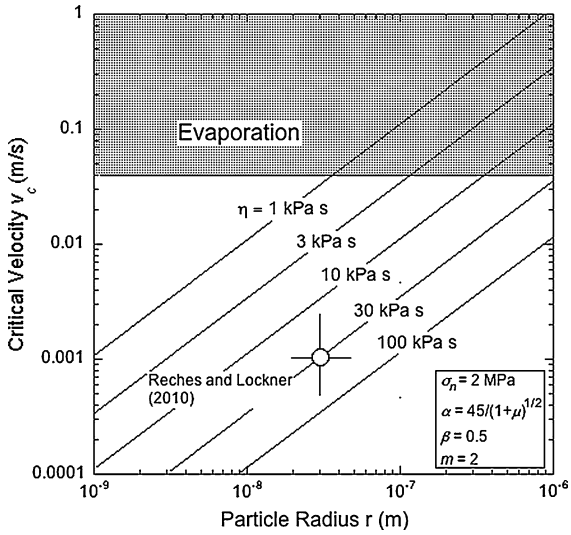

Figure 6
The critical velocity at which friction begins to decrease as a function of particle radius for a range of viscosities. The *open circle* shows the critical velocity of approximately 0.001 m/s at which Reches and Lockner (2010) observed their layer of $r = 20$ nm particles to begin to weaken. α and β, (used to parameterize the structure of the force chain network) were chosen such that $\eta = 30$ kPa s when $h = 1$ nm (as measured by Major *et al.* 2006). Note that for particles larger than approximately $r = 1$ μm the critical velocity is so high that the adsorbed water layer would evaporate and the particles would lock. Hence the high-speed weakening phenomenon is limited to submicron particles in this interpretation

In Fig. 6 we plot the critical velocity as a function of grain size for a range of viscosities and grain sizes. Note that the drop in dynamic viscosity observed by Reches and Lockner (2010) and Kitajima *et al.* (2010) requires sub-micron grains. For grain sizes greater than approximately one micron the critical velocity at which weakening is observed is above 0.04 m/s where shear heating begins to destroy the adsorbed water layer (Fig. 1a).

4. The Effect of Normal Stress

Equation (12) provides an additional test of this model. The equation indicates that the critical velocity for weakening (I–II transition; Fig. 1) is linearly proportional to the normal stress; it is thus expected that the weakening velocity would increase with increasing normal stress. Another prediction is related to the velocity of restrengthening (II–III transition, Fig. 1). The restrengthening is attributed here to heat-related dehydration (Reches and Lockner 2010), and as heating-rate is generally proportional to the normal stress, it is expected that restrengthening velocity would decrease with increasing normal stress. The combined outcome of these two predictions is that the "weakness zone" (region II, Fig. 1) should become smaller with increasing normal stress, and maybe disappear at high normal stress.

To test the above prediction, we plotted the friction–velocity relationships for six continuous experiments with rising velocity and σ_n ranging from 1.1 to 6.6 MPa (Fig. 7). This plot includes only those experiments in Fig. 1 with rising velocity, because their thermal history differs from that of experiments with decreasing velocity (Reches and Lockner 2010). For clarity, the "weakness zone" of three experiments (1.3, 3.1, and 6.6 MPa) is shaded below $\mu \approx 0.6$. The plot indicates that:

1. the size of the weakness zone (shaded area) clearly decreases with increasing normal stress, as predicted; and
2. the critical velocity (for both weakening and strengthening) fits only crudely the predictions: general fit for $\sigma_n = 3.1$–6.6 MPa, but poor fit for tests of $\sigma_n = 1.1$–1.3 MPa.

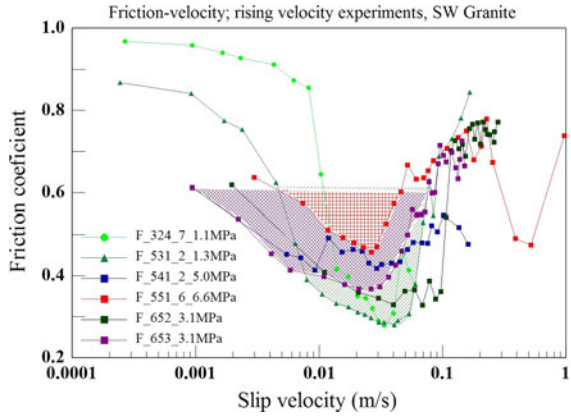

Figure 7
Six continuous experiments from Fig. 1 with increasing velocity and σ_n ranging from 1.1 to 6.6 MPa. The "weakness zone" of three experiments with $\sigma_n = 1.3$, 3.1, and 6.6 MPa is *shaded* below $\mu \approx 0.6$. Note the general decrease in the weakness zone with increasing normal stress

We note however that Eq. (12) includes variables that are not experimentally controlled; e.g., the water layer viscosity (that is very sensitive to the humidity), the grain-size distribution (which is assumed to be constant), and the force chain architecture (α and β). The unknown variations of these variable certainly affect the critical velocity in addition to the net effect of σ_n.

5. Grain Growth

With fragment sizes of the order of tens of nanometers and friction-generated temperatures approaching 500°C, one might expect significant grain growth during these experiments. However, in their analysis of the formation and longevity of nanometer-sized fragments in fault zones, Sammis and Ben-zion (2008) estimated that the time required for a 10 nm quartz particle under wet conditions to double its size was approximately 0.1 s at 1,000°C, 20 s at 800°C, 7 h at 600°C, and 46 days at 500°C (the maximum temperature observed by Reches and Lockner (2010). It seems unlikely that grain growth plays a significant role in the strengthening observed at high slip velocities.

6. Summary and Discussion

The minimum value of friction recently observed in layers of submicron particles does not seem to be caused by the mechanisms usually proposed to explain low friction in similar high-speed experiments. Flash melting at asperities (Rice 2006) is unlikely because of the large transient sliding displacement observed to precede weakening. Thermal pressurization (Rice 2006) seems unlikely because the weakening occurs at temperatures well below 100°C. Silica gel formation (Goldsby and Tullis 2002) does not seem likely because new particles are continuously formed throughout the experiment. These considerations, and the reversibility of the phenomenon, led Reches and Lockner (2010) to propose that the observed weakening was associated with their measurement of a 1 nm layer of water adsorbed by the particles. To test this hypothesis, we have used lubrication theory to estimate the extrusion time of a 1 nm layer from the contact between spherical grains of a given radius. We then compare this extrusion time with the average contact time between particles in one of the grain bridges that are known to support loads in a granular mass. The largest uncertainty in this calculation is the structure of the network of grain bridges (force chains), which affects both the average contact time and the average force between the particles in a chain. We introduce adjustable parameters α and β to characterize the force chain network and use experimental results to estimate their values.

The viscosity of the first few monolayers of adsorbed water is seven orders of magnitude higher than the nominal viscosity. A four monolayer thick film between two quartz surfaces has a measured viscosity of 30 kPa s, whereas an eight monolayer thick film has a measured viscosity of 8.6×10^{-4} Pa s, equal to the nominal viscosity of water.

The most significant quantitative prediction made by this model is the slip velocity at which weakening begins, which we call v_c (the boundary between regions I and II in Fig. 1a). The predicted value of v_c depends on:

1. the size of the smallest particles;
2. the normal stress;
3. the thickness and viscosity of the adsorbed water layer;
4. the distribution of forces carried by the force chains; and
5. the architecture of the force chain network which determines the average lifetime of contact.

Although the size of the smallest particles, the normal stress, and the viscosity of the adsorbed layer are reasonably well known, the other parameters have large uncertainties. The distribution of forces and architecture of the force chains is only crudely known. A reasonable estimate of α and β for the experiments by Reches and Lockner (2010) predicts a value of v_c consistent with the minimum grain size and viscosity of a 1 nm layer of adsorbed water between the grains (Fig. 6). However, the large uncertainties make this more of a plausible argument than a validation of the model.

Having said that, the model does make testable predictions. For example, identification of transition

region III with evaporation of the adsorbed water is supported by Reches and Lockner (2010) measurement of temperatures in excess of 120°C in this regime. Also, all the mechanisms proposed here are reversible, as are the experimental data. Predictions yet to be experimentally tested include the disappearance of weakening under ultra-dry conditions, or when the particle radius exceeds approximately one micron, or at high vales of the normal stress.

References

Abe, S. and K. Mair (2009), *Effects of gouge fragment shape on fault friction: new 3D modeling results*, Geophys. Res. Lett., *36*, L23302, doi:10.1029/2009GLo4o684.

Asay, D. B. and S. H. Kim (2005), *Evolution of the adsorbed water layer structure on silicon oxide at room temperature*, J. Phys. Chem. B, *109,* 16760–16763.

Ben-Zion, Y. and C.G. Sammis (2003), *Characterization of fault zones*, Pure Appl. Geophys., *160*, 677-715.

Brown, E. and H. M. Jaeger (2009), *Dynamic jamming point for shear thickening suspensions*, Phys. Rev. Let., *103*, 086001.

Chester, J.S., F. M. Chester, and A. K. Kronenberg (2005), *Fracture surface energy of the Punchbowl fault, San Andreas system*, Nature, *437*, 133–136. doi:10.1038/nature03942.

Di Toro, G., D. L. Goldsby and T. E. Tullis (2004), *Friction falls towards zero in quartz rock as slip velocity approaches seismic rates*, Nature, *427*, 436–439.

Dienes, G. J. and H. F. Klemm, 1946, *Theory and Application of the Parallel Plate Plastometer*, J. Appl. Phys., *17*, 458–471.

Goldsby, D.L., and T.E. Tullis (2002), *Low frictional strength of quartz rocks at subseismic slip rates*, Geophys. Res. Lett., *29*, 1844. doi:10.1029/2002GL015240.

Han, R., T. Shimamoto, T. Hirose, J.-H. Ree, and J.-i. Ando(2007),*Ultralow friction of carbonate faults caused by thermal decomposition*, Science, *316*, 878–881. doi: 10.1126/science.113976.

Israelachvili, J. N. (1986), *Measurement of the viscosity of liquids in very thin films*, J. Colloid Interface Sci. *110*, 263.

Kamien, R. D. and A. J. Liu (2007), *Why is Random Close Packing Reproducible?*, Phys. Rev. Let., *99*, 155501.

Kitajima, H., J. S. Chester, F. M. Chester, T. Shimamoto (2010), *High-speed friction of disaggregated ultracataclasite in rotary shear: characterization of frictional heating, mechanical behavior, and microstructure evolution*, J. Geophys. Res., *115*, B08408. doi:10.1029/2009JB007038.

Li, T.-D., J. Gao, R. Szoszkiewicz, U. Landman, and E. Riedo (2007), *Structured and viscous water in subnanometer gaps*, Phys. Rev. B., *75*, 115415–115421. doi:10.1103/PhysRevB.75.115415.

Major, R. C., J. E. Houston, M. J. McGrath, J. I. Siepmann, and X.-Y. Zhu (2006), *Viscous water meniscus under nanoconfinement***,** Phys. Rev Let., *96*, 177803.

Mueth, D. M., H. M. Jaeger, and S. R. Nagel (1998), *Force distribution in a granular medium*, Phy. Rev. E, *57*, 3164, 1998.

Reches, Z. and D. A. Lockner (2010), *Fault weakening and earthquake instability by powder lubrication*, Nature, *467*, 452–455, 2010.

Rice, J. R., *Heating and weakening of faults during earthquake slip*, J. of Geophys. Res, *111*. doi:10.1029/2005JB004006.

Sammis, C. G. and Y. Ben-Zion (2008), *The Mechanics of Grain-Size Reduction in Fault Zones*, J. Geophys. Res., *113*. doi: 10.1029/2006JB004892.

Spray, J. G. (2010), *Frictional Melting Processes in Planetary Materials: From Hypervelocity Impact to Earthquakes*, Annu. Rev. Earth Planet. Sci., *38*, 221–254.

Tsutsumi, A., and T. Shimamoto (1997), *High-velocity frictional properties of gabbro*, Geophys. Res. Lett., *24*, 699–702.

(Received July 23, 2010, revised March 30, 2011, accepted March 31, 2011, Published online May 27, 2011)